ARTICLE IN PRESS

Kafkas Universitesi Veteriner Fakultesi Dergisi
Journal Home-Page: http://vetdergikafkas.org
E-ISSN: 1309-2251

Kafkas Univ Vet Fak Derg
xx (xx): xx-xx, 2024
DOI: 10.9775/kvfd.2024.32776

RESEARCH ARTICLE

Morphological and Molecular Changes in Renal Tissue Following Experimental Unilateral Ureteral Obstruction in Rat Kidneys

Tuncer KUTLU [1 (*)] Huseyin OZKAN [2] Ziya YURTAL [3] Ufuk KAYA [4] Mehmet GUVENC [5]

[1] Hatay Mustafa Kemal University, Faculty of Veterinary Medicine, Department of Pathology, TR-31300 Hatay - TÜRKİYE
[2] Hatay Mustafa Kemal University, Faculty of Veterinary Medicine, Department of Genetics, TR-31300 Hatay - TÜRKİYE
[3] Hatay Mustafa Kemal University, Faculty of Veterinary Medicine, Department of Surgery, TR-31300 Hatay - TÜRKİYE
[4] Hatay Mustafa Kemal University, Faculty of Veterinary Medicine, Department of Statistics, TR-31300 Hatay - TÜRKİYE
[5] Hatay Mustafa Kemal University, Faculty of Veterinary Medicine, Department of Physiology, TR-31300 Hatay - TÜRKİYE

(*) **Corresponding authors:**
Tuncer KUTLU
Phone: +90 326 245 5313
E-mail: tuncerkutlu@mku.edu.tr

How to cite this article?

Kutlu T, Ozkan H, Yurtal Z, Kaya U, Guvenc M: Morphological and molecular changes in renal tissue following experimental unilateral ureteral obstruction in rat kidneys. *Kafkas Univ Vet Fak Derg,* 2024 (Article in Press). DOI: 10.9775/kvfd.2024.32776

Article ID: KVFD-2024-32776
Received: 06.08.2024
Accepted: 31.10.2024
Published Online: 12.11.2024

Abstract

This study was designed to investigate the pathological, molecular, and biochemical changes subjected to experimental unilateral ureteral obstruction (UUO) during the acute phase, specifically within a seven-day period. The kidney's reaction to obstructions, such as unilateral ureteral obstruction (UUO), is highly complex and involves a dynamic interplay of various molecular processes. A total of 72 Wistar Albino rats were divided into nine groups, each consisting of eight rats. The left kidneys of the first seven groups underwent UUO surgery, with one group being necropsied daily. All left kidneys were examined using histopathological, immunohistochemical, biochemical, and molecular methods. On the first day of unilateral ureteral obstruction (UUO), significant pathological and biochemical changes were observed in the kidneys. These included the formation of cystic dilated tubules, a decrease in cyclooxygenase-2 (COX-2) gene expression, and a reduction in glutathione peroxidase (GSH-Px) levels. By the second day, hyperemia, increased tumor necrosis factor-alpha (*TNFα*) gene expression, and elevated malondialdehyde (MDA) levels were evident. In the third day; there was mild interstitial mononuclear cell infiltration roteinaceous filtrate in tubules, heightened transforming growth factor beta 1 (TGF-β1) gene and protein expression, and increased angiotensin II (ANG-II) and interleukin-10 (IL-10) protein expression. By day five, kidneys subjected to UUO exhibited hydropic degeneration, TNF-α protein expression, and anti-RELA antibody expression. On the sixth day, significant increase in *IL-10* gene expression was noted. In conclusion; these results provide valuable insights for future studies on UUO pathogenesis and research into potential treatment modalities.

Keywords: Angiotensin II, Interleukin-10, Oxidative stress, Transforming growth factor beta 1, Unilateral ureteral obstruction

Introduction

Ureteral obstructions results in kidney enlargement due to urine accumulation in the renal pelvis or calyces [1-3]. When left untreated, these highly complicated obstructions can lead to hydronephrosis and gradual deterioration of kidney function [1,3,4].

The UUO model serves as a standard for comprehending the origins and mechanisms of renal interstitial fibrosis in mice and rats, with manifestation in mice within a week and rats within 2-3 weeks [1,5,6]. In response to mechanical stress, ligated kidney tissses in the UUO model synthesize chemoattractants within the first 4 hours, triggering interstitial monocyte and T lymphocyte infiltration. These infiltrating cells further exacerbate the disease by synthesizing transforming growth factor beta 1 (TGF-β1), diminishing renal blood flow, and reducing glomerular filtration rates [7].

Proinflammatory cytokines, Nuclear factor kappa B (NF-κB) activation, and oxidative stress are key drivers in progressive renal damage caused by obstructive nephropathy. They induce tubular cell apoptosis and interstitial fibrosis. Increased angiotensin II (ANG-II) production, heightened oxidative stress, and elevated pro-inflammatory cytokines contribute to NF-κB activation. This, in turn, prompts the expression of adhesion molecules and chemokines responsible for leukocyte

recruitment, along with an overexpression of cytokines that intensify the inflammatory response in the damaged kidney [6,8,9].

The UUO model has been studied in the context of chronic kidney diseases, typically spanning around 7 days or extending to 14 days or more [1,3]. The present study investigated the daily changes occurring in rat kidneys subjected to experimental UUO, employing histopathological, immunohistochemical (Anti-RELA), biochemical [oxidative stress, angiotensin II (ANG II), NF-κB, interleukin-10 (IL-10), TGF-β1, tumor necrosis factor-alpha (TNF-α)], and molecular [expression levels of cyclooxygenase-2 (*COX-2*), *TGF-β1*, *TNFα*, *IL-10* genes] methods over a week.

Materials and Methods

Ethical Statement

This study was approved by the Hatay Mustafa Kemal University Animal Experiments Local Ethics Committee (Approval no: 2022/03-02).

Animals and Experimental Protocol

In this study, 72 male Wistar Albino rats, aged 3 months and weighing between 300-350 g, were utilized. Rats were kept under constant environmental conditions (12 h day/night cycles, 24±3°C), received the standard commercial rat food (pellet feed) and had free access to tap water. The rats were divided into 9 groups, each comprising 8 rats. To induce hydronephrosis, the first seven groups underwent UUO surgery, with necropsies conducted on one group daily (day 1: Group 1; day 2: Group 2; day 3: Group 3; day 4: Group 4; day 5: Group 5; day 6: Group 6; day 7: Group 7). The sham group (Group 8) had their abdominal cavity opened and closed without creating UUO and was euthanized on the 1st day. The control group (Group 9) was euthanized on the 1st day without any intervention.

During the UUO procedure for hydronephrosis induction, all rats were anesthetized using xylazine HCL [10 mg/kg, intraperitoneal (IP)] and ketamine HCL (50 mg/kg, IP). The abdominal areas of the anesthetized rats were shaved, and the incision areas were made aseptic while the rats were positioned supinely. Following a midline incision, access to the abdominal cavity was achieved. After exposing the left kidney, the left ureter was identified. Two ligatures with 5/0 non-absorbable thread were placed on the midline of the left ureter during the procedure, and the ureter was cut between the two ligatures. Subsequently, the peritoneum, muscles, and skin were closed routinely using 3/0 absorbable sutures [5].

Finally, the rats were euthanized under xylazine HCL (10 mg/kg, IP) and ketamine HCL (50 mg/kg, IP) anesthesia, and kidney tissues were collected after necropsy.

Histopathological Analysis

Following the experiment, a portion of the left kidney was preserved in 10% buffered formalin for subsequent pathological examination. The samples were washed under tap water, dehydrated in ascending grades of ethanol (70, 80, 90, 96 and 100%), cleared in xylene, and embedded in paraffin. Kidney sections of 4 µm thickness were prepared and stained with haematoxylin and eosin (H&E) for morphological changes. Histopathological alterations, such as mononuclear cell infiltration and cystic dilated tubules in the kidneys, were assessed in five randomly selected areas (at 100x magnification), adhering to the criteria described by Otunctemur et al.[10] and Hassan et al.[9]: 0 denoting no change, 1 indicating changes affecting <25% of the area, 2 signifying changes affecting 25-50% of the area, and 3 representing changes affecting >50% of the area.

Immunohistochemical Analysis

For immunohistochemical analysis, tissue sections were derived from the same blocks utilized in the histopathological examination and placed on adhesive slides. Avidin-Biotin Peroxidase Complex (ABC) technique was performed according to the manufacturer guidelines (SensiTek HRP, ScyTek Laboratories, Logan, UT) to show the expression and localization of anti-RELA in tissues. Paraffin-embedded kidney sections were deparaffinised, hydrated and incubated with 3% H_2O_2 to block peroxidase activity. Proteinase K (Abcam, ab64220) was applied as antigen retrieval to the paraffin sections. Afterward, the sections incubated with anti-RELA antibody [ST.Johns Laboratorıes, STJ94473-100, Anti-RELA antibody (220-300), 1/100 dilution, 45min/45°C]. The binding sites of antibody were visualized with 3,3'-diaminobenzidine tetrahydrochloride (DAB, ScyTek Laboratories, Logan, UT). The samples were counterstained with H&E. Immunohistochemical grading of kidney tissues followed the methodology established by Hassan et al.[9], utilizing a scoring system of 0, 1, 2, and 3.

Molecular Analysis

Post-sacrifice, kidney tissues were promptly washed with PBS solution (pH: 7.4), then placed in nuclease free tubes and frozen in liquid nitrogen. Upon arrival at the laboratory, the frozen samples were stored at -80°C until molecular analysis. For gene expression analyses, total RNA was isolated from kidney tissues using the modified Trizol method through the Hibrizol kit (Hibrigen, TÜRKİYE) [11]. For this purpose, approximately 50 mg of tissue was homogenized in 1 mL Hibrizol in 2 mL nuclease-free tubes using the Bioprep-6 homogenizer (AllSheng, CHINA). The RNA pellet was obtained through successive steps involving chloroform, isopropyl alcohol, and ethyl alcohol, following the kit protocol. The resulting

RNA pellets were diluted with 20-50 µL of nuclease-free water after approximately 10 min of incubation at room temperature. Purity (A260/A280) and concentration values of the isolated RNAs were assessed via SMA-1000 Spectrophotometer (Merinton, CHINA), and their quality was electrophoretically validated through 1% agarose gel electrophoresis.

The isolated RNA samples were adjusted to a concentration of 1000 ng/µL with nuclease-free water and subsequently treated with DNase I (EN0521, Thermo Scientific, USA) to eliminate potential DNA contamination. cDNA synthesis was carried out using the Onescript Plus cDNA Synthesis Kit (G236, ABM, CANADA) following the kit protocols. For this process, samples were incubated in a thermal cycler (BioRad T100, USA) at 55°C for 15 min and at 85°C for 5 min. After the reaction, the samples were completed to 200 µL with nuclease-free water and stored at -80°C until qPCR analysis.

Expression levels of *TNFα, COX-2, TGFβ-1,* and *IL-10* genes were determined by qPCR (Rotorgene Q MDx 5plex HRM, Qiagen USA) with the EnTurbo™ SYBR Green PCR SuperMix kit (EQ014, ELK Biotechnology, China). The *ACTB* were used as the housekeeping gene to determine the expression levels of the target genes, and all samples were analyzed in duplicate. qPCR reaction conditions were set at 15 sec at 95°C, 60 sec at 60°C, and 30 sec at 72°C for 40 cycles, following a 10 min incubation at 95°C. The forward and reverse sequences of the primers used for gene amplification are detailed in *Table 1*.

Biochemical Analysis

Protein analyses for ANG-II, NF-κB, IL-10, TGF-β1, and TNF-α in kidney tissue were conducted using an ELISA plate reader (Bio-Tek, Winooski, VT) and commercial kits (ELK BIOTEK), as per the manufacturer's specified protocol.

For analyses related to oxidative stress and antioxidant activity, tissue samples underwent a 1/10 dilution with Tris buffer (pH 7.4) and were subsequently homogenized using a homogenizer. The determination of total protein in the tissue followed the Lowry method [17].

The assessment of lipid peroxidation (LPO) levels relied on measuring the amount of malondialdehyde (MDA) produced in the tissue. MDA levels were determined according to the spectrophotometric method described by Placer et al.[18]. The pink complex formed by MDA with thiobarbituric acid was measured spectrophotometrically at 532 nm, and the MDA level was expressed as nmol/g protein.

The of glutathione (GSH) levels was determined using the method described by Sedlak and Lindsay [19]. The color intensity of the yellow complex formed as a result of the reaction of 5,5-dithiobis [2-nitrobenzoic acid] with sulfhydryl groups was measured spectrophotometrically at 412 nm and GSH levels were expressed as nmol/g, with the color intensity being directly proportional to the GSH concentration in the medium.

Catalase (CAT) activity in the tissue was assessed according to the method established by Goth, [20]. Tissue incubation with a substrate containing hydrogen peroxide (H2O2) resulted in the breakdown of H2O2 into H2O and O2 through catalase activity. The addition of ammonium molybdate to the medium terminated the reaction. The color change during this process was measured spectrophotometrically against a blank at 405 nm, and catalase enzyme activity was expressed as kU/g protein.

Glutathione peroxidase (GSH-Px) activity in the tissue was determined using the method described by Lawrence and Burk [21]. The yellow color complex formed by the samples with DTNB solution was measured on a spectrophotometer at 412 nm, with GSH-Px enzyme activity expressed as IU/g protein.

Table 1. *Forward and reverse sequences of studied genes*

Genes	Forward and Reverse Primer Sequences	Product length	References
ACTB	F: 5'-TGACAGGATGCAGAAGGAGA-3'	104	[12]
	R: 5'-TAGAGCCACCAATCCACACA-3'		
TNF-α	F: 5'-ACTGAACTTCGGGGTGATCG-3'	153	[13]
	R: 5'-GCTTGGTGGTTTGCTACGAC-3'		
COX-2	F: 5'-TGTATGCTACCATCTGGCTTCGG-3'	94	[14]
	R: 5'-GTTTGGAACAGTCGCTCGTCATC-3'		
TGFβ-1	F: 5'-ATTCCTGGCGTTACCTTGG-3'	117	[15]
	R: 5'-CCTGTATTCCGTCTCCTTGG-3'		
IL-10	F: 5'-TTGAACCACCCGGCATCTAC-3'	91	[16]
	R: 5'-CCAAGGAGTTGCTCCCGTTA-3'		

Statistical Analysis

Before performing the statistical analysis, the parameters were assessed for parametric test assumptions. The Shapiro-Wilk test was used to assess the assumption of normality, and the Levene test was used for homogeneity of variances. Differences in ELISA parameters, histopathological and immunohistochemical findings between groups were determined using the Kruskal-Wallis test. In instances where a significant difference was observed, the multiple Dunn test was used as a post-hoc test. Differences in stress parameters between groups were evaluated with one-way analysis of variance (ANOVA). When a significant difference was revealed, the Tukey test was performed as a post-hoc test. The Spearman correlation coefficient was used to determine the strength and direction of relationships between ELISA and stress parameters. All statistical analyses were performed using the IBM SPSS 23.0 statistical software, and the significance threshold was set at $P<0.05$.

The 2-ΔΔCt method was used to calculate the relative expression levels of target genes in the study and the change in gene expression levels in the groups was presented as fold change compared to the control group [22].

Results

Macroscopically, the kidneys in the control and sham groups appeared normal. However, as the duration of obstruction increased in the UUO groups, the color of these kidneys became lighter, and their volume increased. Particularly on the 6th and 7th days, a significant enlargement of the renal pelvis and the development of hydronephrosis were evident *(Fig. 1)*.

Fig 1. Enlargement of the renal pelvis on the 6th day

Microscopically, the histopathological findings and their scoring are in *Table 2*. Kidneys in the control and sham groups maintained a normal histological structure *(Fig. 2-A)*. In contrast, those subjected to experimental UUO showed statistically significant cystic dilated tubules with mild severity on the 1st day, progressing to moderate severity by the 6th day *(Fig. 2-B,C)*. The vascular hyperemia became less pronounced from the 2nd day onwards *(Fig. 2-D)*. Mononuclear cell infiltration and proteinaceous filtrate in the tubules were evident on the 3rd day *(Fig. 2-E)*. Notably, degenerative changes like hydropic degeneration were observed only on the 5th day, with a statistically significant difference in severity *(Fig. 2-F)*.

Table 3 presents the levels of anti-RELA antibody expression in the groups. Anti-RELA antibody expression

Table 2. *Histopathological findings and scoring observed in the groups*

Groups	Cystic Dilated Tubules		Hyperemia		Hydropic Degeneration		Mononuclear Cell Infiltration		Proteinase Filtrate in Tubules	
	Arithmetic Mean	Standard Error	Arithmetic Mean	Standard Error	Arithmetic Mean	Standard Error	Arithmetic Mean	Standard Error	Arithmetic Mean	Standard Error
Control	0.14 ^{A}	0.14	0.00 ^{A}	0.00	0.00 ^{A}	0.00	0.00 ^{A}	0.00	0.00 ^{A}	0.00
Sham	0.00 ^{A}	0.00	0.00 ^{A}	0.00	0.00 ^{A}	0.00	0.00 ^{A}	0.00	0.00 ^{A}	0.00
Day 1	1.00 ^{B}	0.22	0.25 ^{AB}	0.16	0.14 ^{A}	0.14	0.00 ^{A}	0.00	0.14 ^{A}	0.14
Day 2	1.00 ^{BC}	0.31	1.00 ^{B}	0.27	0.33 ^{A}	0.21	0.29 ^{A}	0.18	0.29 ^{A}	0.18
Day 3	1.29 ^{BCD}	0.18	1.00 ^{B}	0.31	0.29 ^{A}	0.18	1.00 ^{B}	0.22	1.14 ^{BC}	0.34
Day 4	1.71 ^{BCD}	0.29	1.00 ^{B}	0.22	0.71 ^{A}	0.29	1.29 ^{B}	0.29	1.00 ^{BC}	0.22
Day 5	1.71 ^{BCD}	0.18	0.88 ^{B}	0.23	1.57 ^{B}	0.20	1.14 ^{B}	0.14	1.14 ^{BC}	0.14
Day 6	2.14 ^{D}	0.14	0.38 ^{AB}	0.26	1.71 ^{B}	0.18	1.57 ^{B}	0.20	1.14 ^{BC}	0.14
Day 7	2.00 ^{CD}	0.22	0.43 ^{AB}	0.20	1.71 ^{B}	0.18	1.14 ^{B}	0.14	1.29 ^{C}	0.18
p	<0.001		<0.001		<0.001		<0.001		<0.001	

^{A,B,C} *Different capital letters in rows indicate statistical significance between groups (P<0.05)*

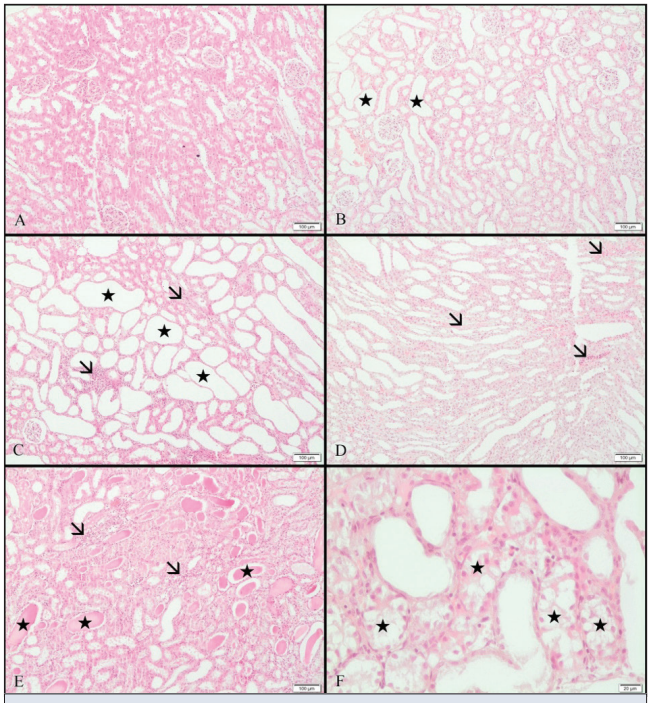

Fig 2. Histopathological changes in the kidneys, H&E. **A-** Control group; normal kidney tissue; **B-** Day 1; slightly cystic dilated tubules *(stars);* **C-** Day 6; cystic dilated tubules *(stars)* and mononuclear cell infiltration *(arrows);* **D-** Day 2; mild hyperemia of the kidneys *(arrows);* **E-** Day 3; proteinaceous filtrate *(stars)* and mononuclear cell infiltration *(arrows)* in tubules; **F-** Day 5; hydropic degeneration (stars) in tubular epithelium

Table 3. *Anti-RELA antibody expression levels in groups*

Groups	Arithmetic Mean	Standard Error
Control	0.14 ^{A}	0.14
Sham	0.00 ^{A}	0.00
Day 1	0.00 ^{A}	0.00
Day 2	0.14 ^{A}	0.14
Day 3	0.14 ^{A}	0.14
Day 4	0.00 ^{A}	0.00
Day 5	0.86 ^{B}	0.14
Day 6	1.14 ^{B}	0.14
Day 7	1.00 ^{B}	0.00
p	<0.001	

^{A,B,C} *Different capital letters in rows indicate statistical significance between groups (P<0.05)*

was negative in the control and sham groups *(Fig. 3-A,B)*. The first statistically significant positivity was detected in the glomeruli and intertubular regions on the 5th day *(Fig 3-C,D)*.

Fig. 4 summarizes the levels of oxidative stress and antioxidant activity markers obtained as a result of the study. The MDA level was significantly elevated on the 2nd day, as well as on the 6th and 7th days, when compared to

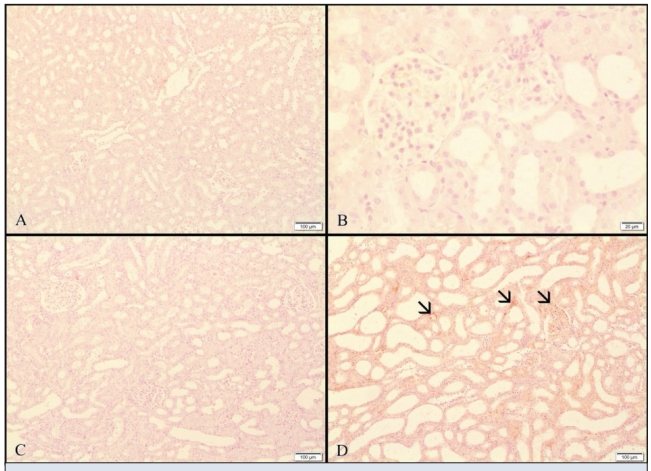

Fig 3. Immunohistochemical staining for Anti-RELA antibody. **A-** Control group; Anti-RELA antibody expression negative; **B-** Day 1; Anti-RELA antibody expression negative; **C-** Day 3; Anti-RELA antibody expression negative; **D-** Day 5; slight Anti-RELA antibody expression in glomeruli and intertubular regions

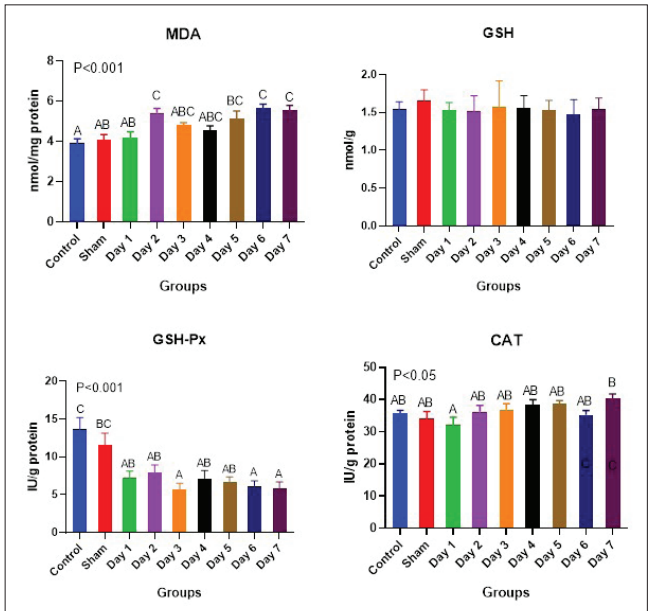

Fig 4. MDA, GSH, GSH-Px, and CAT levels in groups

the control and sham groups. GSH-Px level consistently showed a statistically lower value compared to the control group from the first day. After the 3rd day, it was also lower than the sham group. No significant differences were observed in terms of GSH and CAT compared to the control and sham groups.

Expression levels of the studied genes were significanly changed in different days of experiment. While *TNFα* gene expression levels were consistently higher than in the control and sham groups after the 2nd day, *COX-2* gene expression levels were decrased from day1 to day 5 compared to control (P<0.05). On the other hand, *TGF-β1* gene expression levels were incresed from day 3 (P<0.05). Notably, IL-10 gene expression was significantly higher on the 6th and 7th days compared to the control *(Fig. 5)*.

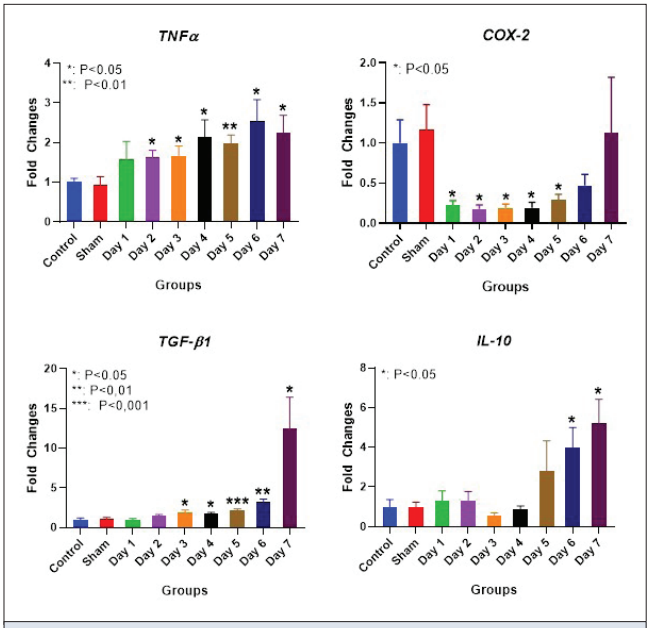

Fig 5. Expression levels of TNFα, COX-2, TGF-β1, and IL-10 genes

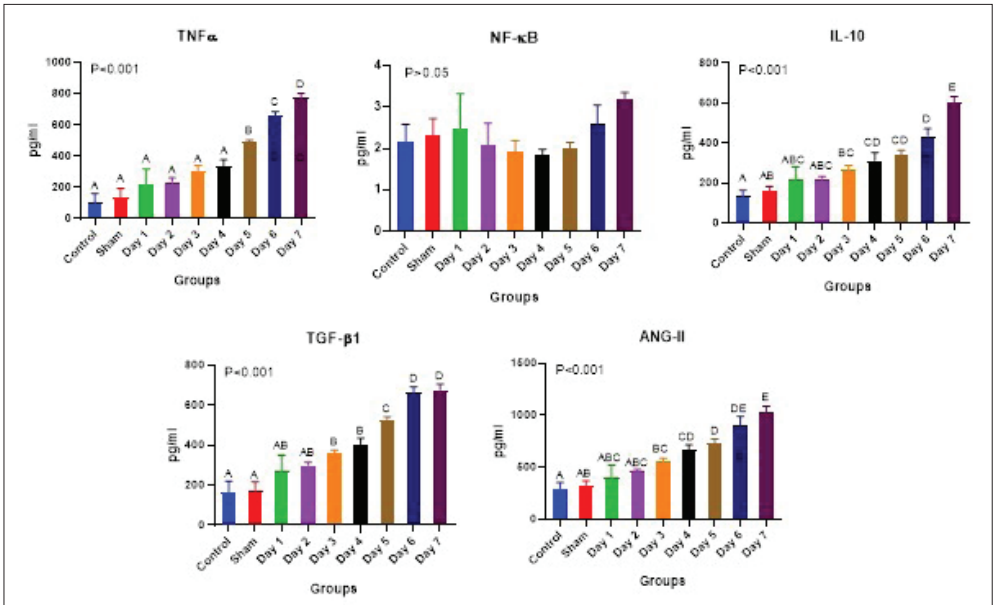

Fig 6. The protein expression levels of TNFα, NF-κB, IL-10, TGF-β1, and ANG-II

Table 4. *Correlation between biochemical parameters and proteins*

Parameters	IL-10	NF-κB	TGF-β1	TNF-α	ANG-II	MDA	GSH	GSH-Px	CAT
IL-10	1	0.353**	0.927***	0.935***	0.970***	-0.476***	0.128	0.485***	-0.090
NF-κB		1	0.259	0.381**	0.338*	-0.118	0.049	0.271*	0.016
TGF-β1			1	0.954***	0.955***	-0.596***	0.189	0.523***	-0.257
TNF-α				1	0.940***	-0.575***	0.183	0.518***	-0.166
ANG-II					1	-0.514***	0.142	0.512***	-0.127
MDA						1	-0.259	-0.397**	0.215
GSH							1	0.073	0.005
GSH-Px								1	-0.062
CAT									1

**P<0.05; **P<0.01; ***P<0.001*

Fig. 6 presents the protein expression levels of the groups. There was no significant change in NF-κB protein levels between the groups. However, ANG-II and IL-10 protein expression levels commenced an increase on day 1 compared to the control and sham groups, becoming significantly elevated compared to the control group on the 3rd day and compared to the sham group on the 4th day. TGF-β1 protein expression level began to rise on the first day, with a significant increase on the 3rd day compared to both the control and sham groups. TNF-α protein expression level started to increase on the 1st day, becoming significant on the 5th day compared to the control and sham groups. *Table 4* illustrates the correlation between biochemical parameters and proteins

Discussion

The UUO model is highly effective, inducing multiple pathophysiological changes within a week of obstruction [1,6,23]. Hassan et al.[9] reported observations in rats subjected to the UUO model over two weeks, including interstitial edema, cystic dilated tubules, atrophy in the glomeruli, thickening of the Bowman capsule, and mononuclear cell infiltration. Similarly, our study revealed distinct histopathological changes in the UUO model, with cystic dilated tubules on the 1st day, hyperemia on the 2nd day, mononuclear cell infiltration, and proteinaceous filtrate in the tubules on the 3rd day, and statistically significant hydropic degeneration in the tubule epithelium on the 5th day.

In acute UUO, it has been reported that mononuclear cell infiltration, particularly by macrophages, follows a biphasic increase starting four hours post-obstruction. The first phase involves a continuous increase in mononuclear cell infiltration over the initial 24 hours, followed by a second phase where the infiltration rises to ten times the normal level within three days and continues to increase for up to 14 days [23]. In the current study, mononuclear cell infiltration began on the 2nd day, reached statistical significance on the 3rd day, and maintained similar levels until the 7th day.

Oxidative stress has been identified as a crucial player in the pathogenesis of UUO, with many markers like MDA showing increased levels. Additionally, major protective antioxidant enzymes such as GSH, GSH-Px, and CAT have been found to decrease [9,24]. Similarly, in the current study, MDA levels increased on the 2nd day and on the 6th and 7th days, while GSH-Px levels consistently remained low from the 1st day. However, no significant changes were detected in terms of CAT and GSH compared to the control and sham groups over the 7 days.

Klahr [25] indicated that ANG-II levels increased with oxidative stress in the UUO model. Consistent with this, the present study found a significant increase in ANG-II levels. The protein expression of ANG-II displayed significant increases on the 3rd day compared to the control, on the 4th day compared to the sham, and continued to rise significantly on the 6th day compared to the preceding days.

The heightened expression of ANG-II can trigger NF-κB activation, inducing both direct and indirect oxidative stress. NF-κB can also be activated by various cytokines such as TNF-α and oxidative stress [1,4,6]. However, in our study, no significant change was observed in the NF-κB protein level. Previous immunohistochemical studies have demonstrated the presence of activated NF-κB complexes in various cells within obstructed kidneys, including glomerular, tubulointerstitial, and infiltrated cells [1,6,26].

The NF-κB transcription factor family comprises p50 (NF-kB1), p52 (NF-kB2), p65 (RelA), c-Rel, and RelB [27]. In our study, the first statistically significant anti-RELA expression positivity was detected in the glomeruli and intertubular regions on the 5th day during immunohistochemical examination.

TGF-β1 is a cytokine that plays a crucial role in tissue damage and inflammation in obstructive nephropathy [24,28]. In the present study, TGF-β1 gene expression was significantly higher than in the control and sham groups every day from the 3rd to the 7th day. The protein expression level of TGF-β1 started increasing on the 1st day, with a significant elevation on the 3rd day compared to both the control and sham groups. Subsequently, on the 5th, 6th, and 7th days, protein expression levels continued to rise significantly compared to the preceding days. TGF-β1 is recognized as a potent chemoattractant, and a noteworthy correlation has been identified between the number of interstitial macrophages and cortical TGF-β1 expression in the UUO model [1]. In our study, TGF-β1 exhibited positive correlations with TNF-α, ANG II, and GSH-Px, while a negative correlation was observed with MDA.

It is well-documented that renal TNF-α levels increase in the early stages of UUO [1,26]. Prud'homme et al.[29] reported a significant increase in plasma levels of TNF-α and IL-10 in the UUO model, reaching a peak at 28 days. The upregulation of TNF-α is associated with severe renal inflammation [30,31]. In our study, TNF-α gene expression was consistently higher than in the control and sham groups every day after the 2nd day. The increase in protein expression levels of TNF-α in the control and sham groups was significant on the 5th day. Furthermore, in the subsequent days, protein expression levels continued to rise significantly compared to the previous days.

IL-10 plays a crucial role in suppressing inflammatory processes by inhibiting the activation of inflammatory pathways [32]. In the renal context, IL-10 has demonstrated

efficacy in suppressing the progression of both acute and chronic kidney injury *in vivo* [32,33]. Jin et al.[32] proposed in their study that IL-10 deficiency exacerbated inflammation and fibrosis in obstructive kidney disease. This exacerbation was attributed to the loss of IL-10's inhibitory effects on inflammatory pathways, including the TGF-β1 signaling pathway and the NF-κB signaling pathway. Consequently, IL-10 emerges as a critical negative regulator of renal inflammation and fibrosis [32,33]. In our study, IL-10 gene expression was significantly higher on the 6th and 7th days compared to the control, sham, and other groups. Additionally, the IL-10 protein expression level showed a significant increase compared to the control group on the 3rd day and the sham group on the 4th day.

In vitro evidence suggests that renal COX-2 expression increases in response to pressure, potentially due to endogenous ROS production during ureteral obstruction [2]. However, in our study, COX-2 gene expression was statistically lower between the 1st and 5th days compared to the control and sham groups.

The UUO model closely mirrors obstructive nephropathy, a condition often encountered in clinical settings due to factors such as benign prostatic hypertrophy or kidney stones, resulting in acute and chronic urinary obstruction [28,31]. A comprehensive understanding of kidney's response to such obstructions holds the potential to refine our comprehension of kidney diseases' pathogenesis and facilitate the development of innovative treatments to mitigate kidney damage [8]. For instance, in our study and consistent with prior research, an increase was observed in oxidative stress marker levels during UUO, coupled with a concurrent decrease in enzymes safeguarding the kidney against oxidative stress. Oxidative stress is associated with many factors that trigger the development of kidney diseases, and eliminating oxidative stress in the acute period is an alternative strategy for treating subsequent chronic kidney diseases.

Anti-TNF-α therapy is a well-established intervention for numerous immunoinflammatory diseases, such as rheumatoid arthritis [34]. Investigating the impact of anti-TNF-α therapy on the pathogenesis of UUO against TNF-α, which elevates even in the early stages of UUO, as indicated by our study, warrants further exploration.

IL-10, with its pivotal role in suppressing inflammatory processes, demonstrated significant increases in protein expression on the 3rd day of our study. This suggests that IL-10 may hold therapeutic potential for chronic kidney diseases, a notion supported by similar results reported by Jin et al.[32].

In conclusion, this study day by day documented the molecular, biochemical, and histopathological changes occurring during the first 7 days of the acute period in rats subjected to UUO. These results are poised to guide future investigations into the pathogenesis of UUO and contribute valuable information to ongoing research aimed at developing treatments for UUO.

Declarations

Availability of Data and Materials: The data given in this study may be obtained from the corresponding auther (T. Kutlu) on reasonable request.

Financial Support: This study was financially supported by the Scientific Research Projects Fund of Hatay Mustafa Kemal University (Project number: 22.GAP.025).

Ethical Approval: This study was done with Hatay Mustafa Kemal University Animal Experiments Local Ethics Committee's permission numbered 2022/03-02.

Conflict of Interest: The authors declared that there is no conflict of interest

Declaration of Generative Artificial Intelligence (AI): The authors declare that the article and/or tables and figures were not written/created by AI and AI-assisted technologies.

Author's Contributions: Conceptualization, T.K., H.Ö., Z.Y. and M.G; funding acquisition, T.K., H.Ö., Z.Y., U.K. and M.G ; methodology, T.K and Z.Y.; resources, T.K., H.Ö., Z.Y., U.K. and M.G.; investigation, T.K., H.Ö., Z.Y., U.K. and M.G.; formal analysis, T.K., H.Ö., U.K. and M.G.; writing-original draft preparation, T.K.; writing-review & editing, T.K., H.Ö., Z.Y., U.K. and M.G.; visualization, T.K.. All authors have read and agreed to the published version of the manuscript.

References

1. Grande MT, Pérez-Barriocanal F, López-Novoa JM: Role of inflammation in tubulo-interstitial damage associated to obstructive nephropathy. *J Inflamm,* 7:19, 2010. DOI: 10.1186/1476-9255-7-19

2. Yang T, Li C: Role of COX-2 in unilateral ureteral obstruction: what is new? *Am J Physiol Renal Physiol,* 310 (8): F746-F747, 2016. DOI: 10.1152/ajprenal.00498.2015

3. Abramicheva PA, Semenovich DS, Zorova LD, Pevzner IB, Sokolov IA, Popkov VA, Kazakov EP, Zorov DB, Plotnikov EY: Decreased renal expression of PAQR5 is associated with the absence of a nephroprotective effect of progesterone in a rat UUO model. *Sci Rep,* 13 (1):12871, 2023. DOI: 10.1038/s41598-023-39848-2

4. Wang Y, Deng X, Yang Z, Wu H: Global research trends in unilateral ureteral obstruction-induced renal fibrosis: A bibliometric and visualized study. *Medicine,* 102 (32):e34713, 2023. DOI: 10.1097/MD.0000000000034713

5. Zhao J, Wang L, Cao A, Jiang M, Chen X, Peng W: Renal tubulointerstitial fibrosis: A review in animal models. *J Integr Nephrol Androl,* 2 (3): 75-80, 2015.

6. Martínez-Klimova E, Aparicio-Trejo OE, Tapia E, Pedraza-Chaverri J: Unilateral ureteral obstruction as a model to investigate fibrosis-attenuating treatments. *Biomolecules,* 9 (4):141, 2010. DOI: 10.3390/biom9040141

7. López-Novoa JM, Martínez-Salgado C, Rodríguez-Peña AB, Hernández FJL: Common pathophysiological mechanisms of chronic kidney disease: Therapeutic perspectives. *Pharmacol Therapeut,* 128 (1): 61-81, 2010. DOI: 10.1016/j.pharmthera.2010.05.006

8. Chevalier RL, Forbes MS, Thornhill BA: Ureteral obstruction as a model of renal interstitial fibrosis and obstructive nephropathy. *Kidney Int,* 75 (11): 1145-1152, 2009. DOI: 10.1038/ki.2009.86

9. Hassan NM, Said E, Shehatou GS: Nifuroxazide suppresses UUO-induced renal fibrosis in rats via inhibiting STAT-3/NF-κB signaling, oxidative stress and inflammation. *Life Sci,* 272:119241, 2021. DOI: 10.1016/j.lfs.2021.119241

10. Otunctemur A, Ozbek E, Cakir SS, Dursun M, Cekmen M, Polat EC, Ozcan L, Somay A, Ozbay N: Beneficial effects montelukast, cysteinyl-leukotriene receptor antagonist, on renal damage after unilateral ureteral obstruction in rats. *Int Braz J Urol,* 41 (2): 279-287, 2015. DOI: 10.1590/S1677-5538.IBJU.2015.02.14

11. Rio DC, Ares M, Hannon GJ, Nilsen TW: Purification of RNA using TRIzol (TRI reagent). *Cold Spring Harb Protoc,* 2010 (6):pdb-prot5439, 2010. DOI: 10.1101/pdb.prot5439

12. Kimura Y, Mikami Y, Osumi K, Tsugane M, Oka J, Kimura H: Polysulfides are possible H2S-derived signaling molecules in rat brain. *FASEB J,* 27 (6): 2451-2457, 2013. DOI: 10.1096/fj.12-226415

13. Zhao J, Gao X, Wang A, Wang Y, Du Y, Li L, Li M, Li C, Jin X, Zhao M: Depression comorbid with hyperalgesia: Different roles of neuroinflammation induced by chronic stress and hypercortisolism. *J Affect Disord,* 256, 117-124, 2019. DOI: 10.1016/j.jad.2019.05.065

14. Güvenç M, Cellat M, Özkan H, Tekeli İO, Uyar A, Gökçek İ, İşler CT, Yakan A: Protective effects of tyrosol against DSS-induced ulcerative colitis in rats. *Inflammation,* 42 (5): 1680-1691, 2019. DOI: 10.1007/s10753-019-01028-8

15. Ding S, Yu L, An B, Zhang G, Yu P, Wang Z: Combination effects of airborne particulate matter exposure and high-fat diet on hepatic fibrosis through regulating the ROS-endoplasmic reticulum stress-TGFβ/SMADs axis in mice. *Chemosphere,* 199, 538-545, 2018. DOI: 10.1016/j.chemosphere.2018.02.082

16. Banyatworakul P, Pirarat N, Sirisawadi S, Osathanon T, Kalpravidh C: Efficacy of bubaline blood derived fibrin glue in silk ligature-induced acute periodontitis in Wistar rats. *Vet World,* 14 (10): 2602-2612, 2021. DOI: 10.14202/vetworld.2021.2602-2612

17. Lowry OH, Rosenbrough NJ, Farr AL: Protein measurement with the folin phenol reagent. *J Biol Chem,* 193, 265-275, 1951.

18. Placer ZA, Cushman LL, Johnson BC: Estimation of product of lipid peroxidation (malonyldialdehyde) in biochemical systems. *Anal Biochem,* 16, 359-364, 1966. DOI: 10.1016/0003-2697(66)90167-9

19. Sedlak J, Lindsay RH: Estimation of total, protein-bound, and nonprotein sulfhydryl groups in tissue with Ellman's reagent. *Anal Biochem,* 25, 192-205, 1968. DOI: 10.1016/0003-2697(68)90092-4

20. Goth LA: Simple method for determination of serum catalase activity and revision of reference range. *Clin Chim Acta,* 196, 143-151, 1991. DOI: 10.1016/0009-8981(91)90067-M

21. Lawrence RA, Burk RF: Glutathione peroxidase activity in selenium-deficient rat liver. *Biochem Biophys Res Commun,* 71, 952-958, 1976. DOI: 10.1016/0006-291X(76)90747-6

22. Livak KJ, Schmittgen TD: Analysis of relative gene expression data using real-time quantitative PCR and the $2^{-\Delta\Delta CT}$ method. *Methods,* 25 (4): 402-408, 2001. DOI: 10.1006/meth.2001.1262

23. Nishida M, Hamaoka K: Macrophage phenotype and renal fibrosis in obstructive nephropathy. *Nephron Exp Nephrol,* 110 (1): e31-e36, 2008. DOI: 10.1159/000151561

24. Dendooven A, Ishola DA, Nguyen TQ, Giezen DM, Kok RJ, Goldschmeding R, Joles JA: Oxidative stress in obstructive nephropathy. *Int J Exp Pathol,* 92 (3): 202-210, 2011. DOI: 10.1111/j.1365-2613.2010.00730.x

25. Klahr S: Urinary tract obstruction. *Semin Nephrol,* 21, 133-145, 2001. DOI: 10.1053/snep.2001.20942

26. Esteban V, Lorenzo O, Rupérez M, Suzuki Y, Mezzano S, Blanco J, Kretzler M, Sugaya T, Egido J, Ruiz-Ortega M: Angiotensin II, via AT1 and AT2 receptors and NF-kappaB pathway, regulates the inflammatory response in unilateral ureteral obstruction. *J Am Soc Nephrol,* 15, 1514-1529, 2004. DOI: 10.1097/01.ASN.0000130564.75008.F5

27. Zhang H, Sun SC: NF-κB in inflammation and renal diseases. *Cell Biosci,* 5:63, 2015. DOI: 10.1186/s13578-015-0056-4

28. Klahr S, Morrissey J: Obstructive nephropathy and renal fibrosis: The role of bone morphogenic protein-7 and hepatocyte growth factor. *Kidney Int Suppl,* 87, 105-112, 2003. DOI: 10.1152/ajprenal.00362.2001

29. Prud'homme M, Coutrot M, Michel T, Boutin L, Genest M, Poirier F, Launay JM, Kane B, Kinugasa S, Prakoura N: Acute kidney injury induces remote cardiac damage and dysfunction through the galectin-3 pathway. *JACC Basic Transl Sci,* 4, 717-732, 2019. DOI: 10.1016/j.jacbts.2019.06.005

30. Wen Y, Lu X, Ren J, Privratsky JR, Yang B, Rudemiller NP, Zhang J, Griffiths R, Jain MK, Nedospasov SA: KLF4 in macrophages attenuates TNFα-mediated kidney injury and fibrosis. *J Am Soc Nephrol,* 30, 1925-1938, 2019. DOI: 10.1681/ASN.2019020111

31. Prieto-Carrasco R, Silva-Palacios A, Rojas-Morales P, Aparicio-Trejo OE, Medina-Reyes EI, Hernández-Cruz EY, Pedraza-Chaverri J: Unilateral ureteral obstruction for 28 days in rats is not associated with changes in cardiac function or alterations in mitochondrial function. *Biology,* 10 (7):671, 2021. DOI: 10.3390/biology10070671

32. Jin Y, Liu R, Xie J, Xiong H, He JC, Chen N: Interleukin-10 deficiency aggravates kidney inflammation and fibrosis in the unilateral ureteral obstruction mouse model. *Lab Invest,* 93 (7): 801-811, 2013. DOI: 10.1038/labinvest.2013.64

33. Choi YK, Kim YJ, Park HS: Suppression of glomerulosclerosis by adenovirus-mediated IL-10 expression in the kidney. *Gene Ther,* 10, 559-568, 2023. DOI: 10.1038/sj.gt.3301926

34. Leone GM, Mangano K, Petralia MC, Nicoletti F, Fagone P: Past, present and (foreseeable) future of biological anti-TNF alpha therapy *J Clin Med,* 12 (4):1630, 2023. DOI: 10.3390/jcm12041630